Available online at www.sciencedirect.com

ScienceDirect

Procedia Materials Science 5 (2014) 2376 – 2381

Procedia Materials Science

www.elsevier.com/locate/procedia

International Conference on Advances in Manufacturing and Materials Engineering, AMME 2014

Mechanical Properties and Microstructural Characterization of Friction Stir Welded AISI 316 Austenitic Stainless Steel

Manish P. Meshram, Basanth Kumar Kodli, Suhash R. Dey*

Department of Materials Science and Engineering, Indian Institute of Technology Hyderabad, Ordnance Factory Estate, Yeddumailaram-502205

Abstract

The aim of this work is to check feasibility of joining austenitic stainless steel using friction stir welding (FSW). Defect free weld is observed achieved in 4mm thick austenitic stainless steel friction stir welded with tool rotation speed of 1100 RPM and welding speed of 8 mm/min. The welds are tested mechanically by tensile tests and their Vickers hardness values are measured while their images are obtained by optical microscopy. Nearly equal ultimate tensile strength of the weld with increase of hardness in nugget zone with respect to the base material is achieved.

Selection and peer-review under responsibility of Organizing Committee of AMME 2014

Keywords: AISI-316, Friction Stir Welding, PCBN tool.

1. Introduction

Friction stir welding (FSW) is a solid state joining process invented and patented by The Welding Institute (TWI, UK) (C.J. Dawes et al., 1999). In conventional fusion welding of AISI 304, melting of material takes place in the weld zone which leads to the formation of "sigma phase" and chrome carbide, imparting poor weld quality (C. Meran et al., 2007). The maximum temperature of the weld during FSW is predicted to reach around 0.8 of the melting temperature of the metal (H. K Bhadeshia et al., 2008). In FSW, the joining occurs due to simultaneous frictional heating and deformation of rotating tool without melting and recasting of metal which generate fewer defects as compared to traditional welding processes like fusion welding. In addition, FSW is an eco-friendly and

* Corresponding author. Tel.: +91 (0)40 23016096; fax: +91(0)40 23016032.
E-mail address: suhash@iith.ac.in

Selection and peer-review under responsibility of Organizing Committee of AMME 2014
doi:10.1016/j.mspro.2014.07.482

energy efficient green technique. In the two last decades, significant development in FSW of various materials has happened like successful butt welding of harder materials (R. S. Mishra et al., 2007). The main objective of the present work is to check feasibility of joining of austenitic stainless steel by FSW, analysed through its mechanical properties and microstructure.

2. Experimental

2.1 Materials and Experimental Procedure

As received plates of austenitic stainless steel having dimensions (120mm x 80 mm x 4 mm) with nominal chemical composition (table 1) are obtained. Plates were mechanically ground and milled from the edges. ETA Welding machine capacity 10 ton vertical bed (specifications given in Table 2) at IISc Bangalore was used to friction stir weld the plates with varying welding parameters using polycrystalline cubic boron nitride (PCBN)-tungsten rhenium (WRe) composite tool (obtained from Megastir having commercial name Q70) shown in figure 1 (R. Steel et al., 2011). Tensile samples were cut using electric discharge machine (EDM) (as shown in Figure 2) to evaluate transverse tensile properties and tested on a 30 KN Instron tensile test machine with a strain rate of $10^{-3}s^{-1}$ as per the guide lines of ASTM E8M specification (V. Balasubramanian et al., 2010). Dura Scan 20 Emco-Test Vickers hardness machine with diamond pyramid shaped indenter was used to get hardness profile (0.98N of load for 15 s) at regular interval of 1 mm on the cross section perpendicular to the welding direction of all the welds. Microstructural observations were performed by optical microscopy (OM). The specimens for OM were cut perpendicular to the welding direction by EDM and were mechanically ground with silicon carbide grinding paper (600, 1000, 1500, 2000 grit) and diamond suspension (6, 3 and 1 µm), followed by electropolishing with A3 solution (10% perchloric acid + 30% methanol + 60% butanol) and then etched in methanolic aqua regia for 20 s. Optical microscope (Leica DM 6000M) was used to perform OM.

Table 1. Nominal chemical composition of AISI-316

% C	% Mn	% Si	% Cr	% Ni	% Mo	% P	% S	% Fe
0.003	0-2	0-1	16-18	10-14	2-3	0.045	0.03	balanced

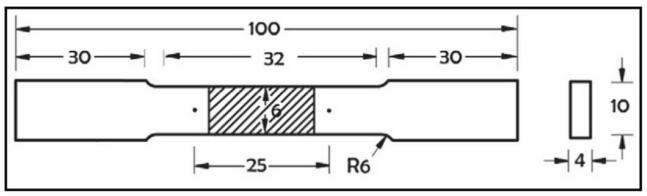

Fig. 2. Tensile Specimen of E8M specification (Dimensions in mm).

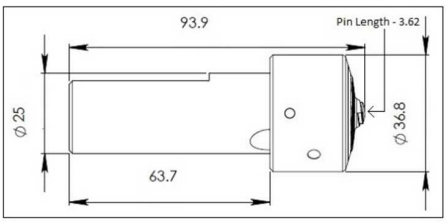

Fig. 1. Megastir tool drawing (Dimensions in mm)

Table 2. ETA friction stir welding machine specifications

	Min.	Max.
Spindle speed	1 RPM	3000 RPM
Welding speed	16 µm/sec	3000 mm/min
Plunge speed	16 µm/sec	2000 mm/min

3. Results and Discussion

3.1 Optimization of Welding Parameters

First to optimize plunge depth, the tool was plunged without any welding speed at 1100 RPM to achieve minimum flash generation. After four trials the plunge depth was optimized as 3.72 mm. In FSW heat generation depends on various factors like rotation per minute (RPM), welding speed (mm/min), friction coefficient of materials, axial force (N), tool tilt angle etc. For all the experimentations the tool tilt angle was kept constant as 2^{o}. The experiments arranged were shown in table 3 with varying RPM and welding speed and characterization were carried out on all the samples to determine the best weld.

3.2 Optical Microscopy

The optical micrograph of the transverse section of the base material is given in figure 3. The base material was obtained as heat treated rolled sheet and consists of equiaxed austenite grains containing several annealing twins.

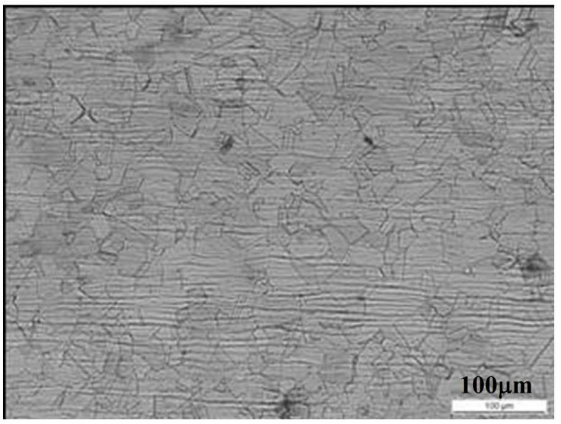

Fig. 3. Optical microscopy of base material

Table 3. Design of experiments

Sr No.	RPM	Welding speed(mm/min)
T1	1100	8
T2	1100	12
T3	1100	16
T4	1000	8
T5	1000	12
T6	1000	16
T7	900	8
T8	900	12
T9	900	16

Transverse section of few welded specimens (T1, T2, T5 and T6) are shown in figure 4.The weld specimens in the transverse section showed mainly the central nugget zone (T1 weld with bottom part containing onion rings like microstructure, figure 4(a)) followed by thermomechanically affected zone (TMAZ). The grains appeared equiaxed and smaller in the nugget zone than in the base material. In all the welds, a clear contrast appeared at around 3-4 mm from the center of the nugget zone between TMAZ and nugget region in the advancing side, stating not proper mixing. The contrast is appeared less in the retreating side. Inside the nugget zone, the material flow lines represent the material being swayed from the advancing side and mixed forcibly into the retreating side, creating smooth transition with no contrast. Except T1 weld, the rest of the welds showed several defects like pores at the bottom of the nugget zone region and few of their transverse section optical images are given in figure 4(b, c and d).

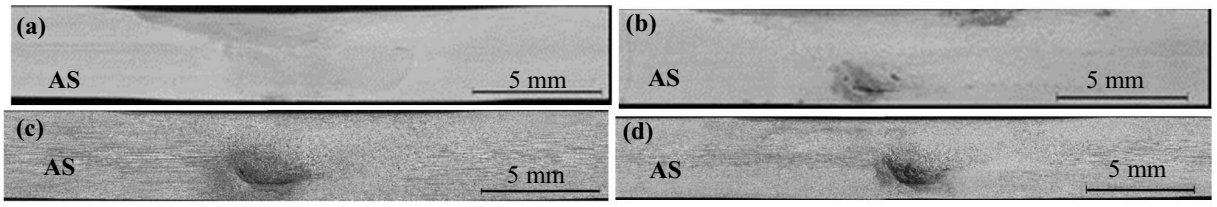

Fig.4. Transverse sections of samples (a) T1 (b) T2 (c) T5 (d) T6 (where AS denotes advancing side)

The optical images at various weld zones of sample T1 are shown in figure 5. Nugget zone and Thermomechanically affected zone (TMAZ) are given in figure 5(a and b). Due to stirring action of tool the grains in the nugget zone (figure 5a) are completely distorted with no twin boundaries as present in the base material. This can be attributed to the thermal and mechanical actions experienced by this material, which caused dynamic recrystallization to occur. Also the grains in TMAZ seem to be larger than the base material.

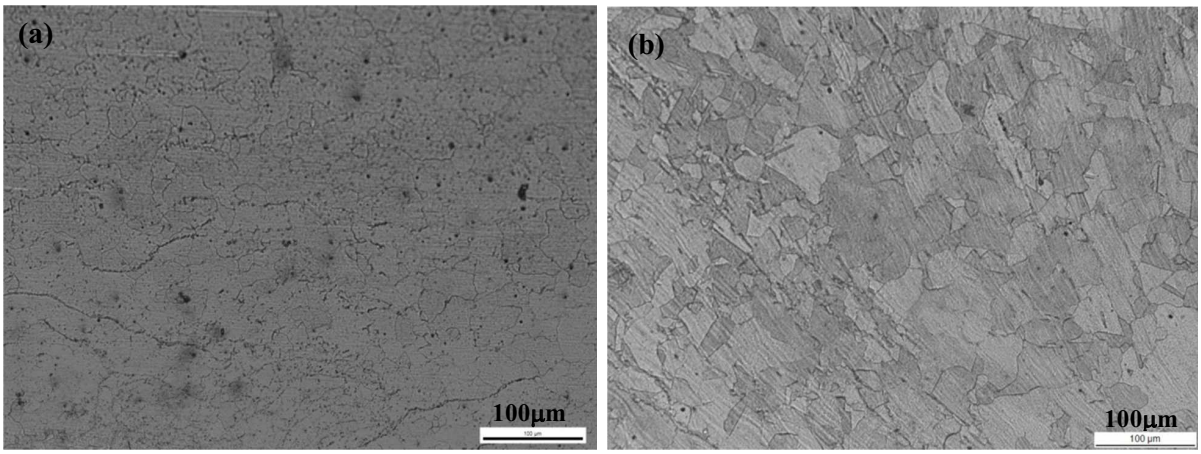

Fig. 5.Various zones in T1 welded sample (a) Nugget Zone (b) TMAZ

3.3 Tensile Test

Tensile tests were performed on the welded samples and the results obtained were compared with the base material. The results are shown in table 4 and few specimen specific graphical plots are given in figure 6. Excellent average 610 MPa UTS value is obtained from the T1 weld, which is just above the base material, with an average elongation of 35%. T1 weld showed necking at around 1.5 cm away from center at the advancing side of the base material region. Except T1, the rest of the welds necked and fractured in the advancing side in between 3-4 mm from the nugget zone (at the nugget zone–TMAZ interface). This is expected with the fact of sudden change in grain microstructure between the nugget zone and TMAZ, becoming the weak region and therefore, failed first under stress. Containing no defects (pores) and smooth transition of grain structure from the nugget zone to the TMAZ and then to the base material, the weld region of T1 (optical images given below) behaves quite similar to the base material and hence, achieved with equal UTS value. Similar values of plastic yield and work hardening behavior in the plastic region between the T1 weld and the base material, suggesting achieving of a good welding condition for this austenitic stainless steel.

Table 4 Tensile results.

Sr. No	RPM	Welding Speed (mm/min)	UTS (MPa)			% Elongation		
			1	2	Average	1	2	Average
T1	1100	8	630	590	610	37	32	35
T2	1100	12	397	345	371	5	1	3
T3	1100	16	343	364	354	3	4	3.5
T4	1000	8	361	443	402	3	7	5
T5	1000	12	428	407	417	5	3	4
T6	1000	16	553	378	465	20	2	11
T7	900	8	365	371	368	3	5	4
T8	900	12	399	412	405	5	2	3.5
T9	900	16	343	318	330	5	1	3
Base Material			608			49		

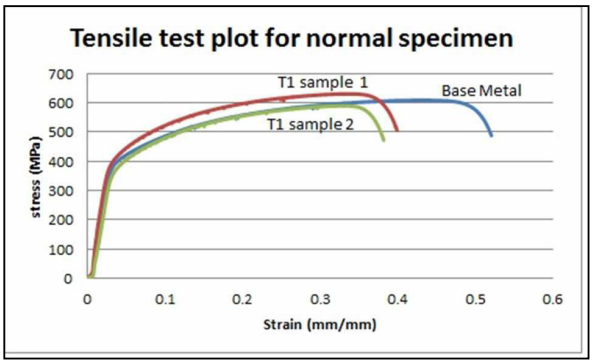

Fig. 6. Plots for tensile test of base material and T1 welded samples.

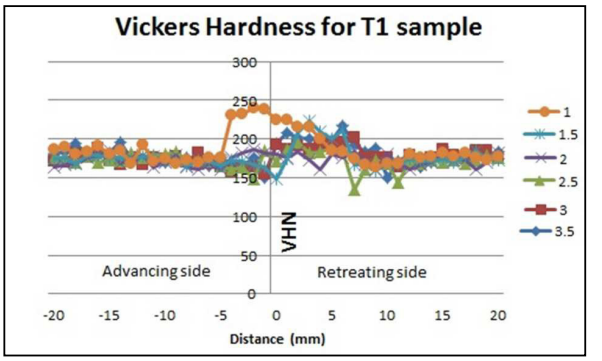

Fig. 7. Vickers hardness profile across the weld. 1, 1.5, 2, 2.5, 3, 3.5 corresponds to distance from top in mm.

3.4 Vickers Hardness

Vickers hardness tests taken on the cross section perpendicular to the welding direction of the base material and all the welds showed nearly no differences among them. The hardness value of 190 VHN is obtained for the base material. The hardness profile of the best weld (T1 weld) at various depths is given in figure 7. The indentation was taken after every 1mm to detect the changes in hardness at various zones. High hardness at the top of the bead in stir zone is observed due to the presence of fine grain structure which arises due to severe thermomechanical deformation of that area by the touching of the tool shoulder. Furthermore, the hardness goes on decreasing as the shoulder effect decreases in the nugget zone. Good increase in hardness value is noticed in the top part of the nugget zone of the T1 weld than that of the base material which is due to the finer grains generated in the nugget zone.

4. Conclusion

The microstructural and mechanical evolution of AISI-316 stainless steel during friction stir welding is studied. A defect free weld is obtained with welding parameters of rotation speed 1100 RPM and welding speed of 8mm/min. Ultimate tensile strength of this welded sample is obtained just above the base material with an increase in hardness in the nugget zone.

Acknowledgement

The authors gratefully acknowledge Professor Satish V. Kailas (Mechanical Engineering, IISc Bangalore, India) for the usage of friction stir welding machine. This research has been funded by DAE, India (No.2012/20/34/1/BRNS).

References

C.J. Dawes, W.M. Thomas, E.D. Nicholas, J.C. Needham,M.G. Murch, and P. Templesmith, 1991 International Patent Application PCT/GB92/02203 and GB Patent Application 9125978.8,.

C. Meran, V. Kovan, A. Alptekin, 2007, Friction stir welding of AISI 304 austenitic stainless steel. Mat.-wiss. u. Werkstofftech. 38, 829-835.

H. K Bhadeshia, D. H., R. Nandan, T. DebRoy, 2008, Recent advances in friction-stir welding - process, weldment structure and properties. Progress in Materials Science 53, 980-1023.

Rajiv S. Mishra, Murray W. Mahoney, 2007. Friction Stir Welding and Processing, ASM International, p 1-5.

R. Steel, S. Packer, 2011.Evaluation of Mechanical Properties of 304L and 316L Stainless Steels Friction Stir Welded. Proceedings of the Twenty-first International Offshore and Polar Engineering Conference. IV: 530-533.

V. Balasubramanian et al, 2010. An assessment of microstructure, hardness, tensile and impact strength of friction stir welded ferritic stainless steel joints. Materials and Design. 3: 4592–4600.